

Low Rate Concatenated Zigzag-Hadamard Codes

Guosen Yue*, W. K. Leung[†], Li Ping[†] and Xiaodong Wang[‡]

*NEC Laboratory America, Inc., Princeton, NJ 08540.

[†]Dept. of Electronic Eng., City University of Hong Kong.

[‡]Dept. of Electrical Eng., Columbia University, New York, NY 10027.

Abstract—We introduce a new class of low-rate error correction codes called concatenated zigzag Hadamard (ZH) codes which are specified by a highly structured zigzag graph with each segment being a Hadamard codeword. The ZH codes enjoy extremely simple encoding and very-low-complexity soft-input soft-output (SISO) decoding. We present an asymptotic performance analysis of the proposed codes using the extrinsic mutual information transfer (EXIT) chart for infinite-length codes. We also provide a union bound analysis of the error performance for finite-length codes.

I. INTRODUCTION

The ultimate Shannon capacity of an additive white Gaussian noise (AWGN) channel is $E_b/N_0 \simeq -1.59$ dB [1]. Since the discovery of turbo codes [2], low-rate concatenated codes have been studied in [3], [4] which offer relatively higher performance but they also incur higher complexity due to the complex trellis structures. The repeat-accumulate (RA) codes [5] have been proved to achieve the Shannon limit in AWGN channels when the code rate approaches zero. The low-density parity-check (LDPC) codes [6], [7], also exhibit capacity-approaching performance for various code rates when the ensemble profiles are optimized [8]. However, in the low-rate region, both RA codes and LDPC codes suffer from performance loss and extremely slow convergence using iterative decoding. Other low-rate codes that have been devised to approach the Shannon limit include [9], [10], [11]. This paper proposes a new class of low-rate codes called concatenated zigzag Hadamard (ZH) codes which are constructed by a highly structured zigzag graph [12] with each segment being a Hadamard codeword. The soft decoding algorithm for the turbo-Hadamard codes [13] can be applied to decode the concatenated ZH codes. The performance of the concatenated ZH codes is close to that of the turbo Hadamard codes [13], but the former enjoy much simpler encoding and decoding structures. We will conduct EXIT chart analysis to predict the performance of very long ZH codes and derive a bounding technique for the performance of short ZH codes. The proposed codes work well in the low-rate region. Simulation results demonstrate that the proposed concatenated ZH codes with long block length achieve 10^{-5} BER at $E_b/N_0 = -1.15$ dB, about 0.44 dB from the ultimate Shannon limit.

II. ZH CODES AND CONCATENATION SCHEMES

A. Hadamard Codes

A Hadamard codeword is obtained from a Hadamard matrix. Starting from $\mathbf{H}_1 = [+1]$, an $n \times n$ ($n=2^r$) Hadamard matrix \mathbf{H}_n

over $\{+1, -1\}$ can be constructed recursively as

$$\mathbf{H}_n = \begin{bmatrix} +\mathbf{H}_{\frac{n}{2}} & +\mathbf{H}_{\frac{n}{2}} \\ +\mathbf{H}_{\frac{n}{2}} & -\mathbf{H}_{\frac{n}{2}} \end{bmatrix}. \quad (1)$$

A length- 2^r Hadamard codeword set is formed by the columns of the bi-orthogonal Hadamard matrix $\pm\mathbf{H}_n$, denoted by $\{\pm\mathbf{h}^j: j=0, \dots, 2^r-1\}$, in a binary $\{0, 1\}$ form, i.e., $+1 \rightarrow 0$ and $-1 \rightarrow 1$. We call r the order of the Hadamard code. Each Hadamard codeword carries $(r+1)$ bits of information. In systematic encoding, the bit indexes $\{0, 1, 2, 4, \dots, 2^{r-1}\}$ are used as information bit positions of the length- 2^r Hadamard code. The other bits are parity bits. Denote \mathcal{H} as a Hadamard encoder. Then, the Hadamard encoding can be represented by $\mathbf{c} = \mathcal{H}(b_0, b_1, \dots, b_r)$. Clearly, the resulting codeword \mathbf{c} is a column of either $+\mathbf{H}_n$ or $-\mathbf{H}_n$. Hereafter, for simplicity we will drop the subscript n in \mathbf{H}_n .

B. Zigzag Hadamard Codes

Similar to the zigzag code [12], a ZH code can be described graphically as shown in Fig. 1. Each *segment* is a length- 2^r Hadamard code. The information bit sequence \mathbf{D} is first segmented into blocks $\mathbf{d}_k = [d_k(1), \dots, d_k(r)]$, $k=1, \dots, K$, represented by the white nodes in Fig. 1. With the last parity bit of the previous segment being the first input bit to the Hadamard encoder for the current segment, the coded bits of the k th segment are obtained by $\mathbf{c}_k = \mathcal{H}(c_{k-1}(2^r-1), d_k(1), \dots, d_k(r))$, where the codeword vector $\mathbf{c}_k = [c_k(0), \dots, c_k(2^r-1)]$ with $c_k(0) = c_{k-1}(2^r-1)$ and $c_k(2^{j-1}) = d_k(j)$, $j=1, \dots, r$. Note that the first segment contains one extra information bit since its first bit can be freely assigned. For convenience, we will ignore the first bit by setting it to zero. Since the first coded bit of each segment is the last bit of the previous segment, we call it a *common bit*, represented by a black node in Fig. 1. All other nodes are parity nodes, represented by the gray nodes. Denote $q_k = c_k(0)$ and let \mathbf{p}_k represent all the parity bits, i.e., $\mathbf{p}_k = \{c_k(i), i \neq 0, i \neq 2^{j-1}, j=1, \dots, r\}$. The coded bit sequence is then denoted by a triplet, i.e., $\mathbf{c}_k = \{\mathbf{d}_k, q_k, \mathbf{p}_k\}$, $\forall k$. Obviously, the above ZH code is a *systematic* code.

We can also construct a *non-systematic* ZH code. The purpose of considering non-systematic ZH codes is to guarantee that the codes contain the recursive nature, which will be elaborated in Section III. First, let

$$\tilde{d}_k(j) = c_{k-1}(2^r-1) \oplus d_k(j), \quad j=1, \dots, r, \quad (2)$$

where \oplus denotes the binary addition. Then, we perform the Hadamard encoding for $\{\tilde{d}_k(j)\}$, i.e., $\mathbf{c}_k = \mathcal{H}(c_{k-1}(2^r-1), \tilde{d}_k(1), \dots, \tilde{d}_k(r))$, where $c_k(2^{j-1}) = \tilde{d}_k(j)$, $j=1, \dots, r$. Denote $\tilde{\mathbf{d}}_k = [\tilde{d}(1), \dots, \tilde{d}(r)]$. The codeword sequence of a

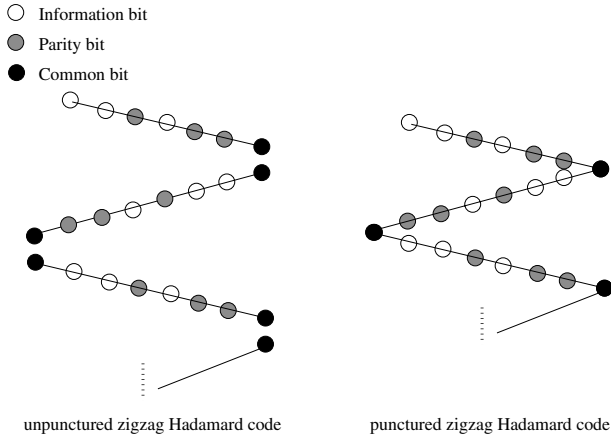


Fig. 1. Graphical representation of a systematic ZH code: $r=3$.

non-systematic zigzag Hadamard code is then given by $\mathbf{c}_k = \{\mathbf{d}_k, \mathbf{q}_k, \mathbf{p}_k\}$, $\forall k$. The code rate for both the systematic and the non-systematic ZH codes is $r/2^r$. Finally we can puncture the common bits $\{q_k\}$ to obtain the punctured ZH code with the code graph shown on the right hand side of Fig. 1. The code rate of this punctured ZH code is $r/(2^r-1)$.

ZH codes are convolutional-like codes and hence can be represented by a two state trellis with four bundles of parallel branches corresponding to the first and the last bit in a Hadamard code segment. Fig. 2 depicts an example of the j th segment of the two-state ZH trellis with $r = 2$, where the codewords associated with the edges are also depicted in the figure with the underlining bits being the systematic bits.

C. Concatenated Zigzag Hadamard Codes

It is easily seen from the code graph in Fig. 1 that the whole code structure does not contain any loop. Therefore, a ZH code can be viewed as an alternative *tree code* described in [14] with the strong Hadamard constraints replacing the single parity check constraints. A concatenated ZH code can be formed based on the coding structure of the concatenated tree (CT) codes [14].

Concatenation of systematic codes: A concatenated systematic code is constructed by parallel concatenating M systematic ZH codes. Let $\{\mathbf{D}, \mathbf{q}, \mathbf{P}\}$ denote the information bits, the common bits, and the parity bits. Denote $\mathbf{D}^{(m)}$ as the m th interleaved version of \mathbf{D} and $(\mathbf{q}^{(m)}, \mathbf{P}^{(m)})$ as the corresponding common and parity bits. The output from each systematic encoder defined in Section II-B contains the triplet sequence $\{\mathbf{D}^{(m)}, \mathbf{q}^{(m)}, \mathbf{P}^{(m)}\}$, $\forall m$. To avoid repeating the information sequence, we only transmit the information bits once, and only collect $\{\mathbf{q}^{(m)}, \mathbf{P}^{(m)}\}$ from the m th component encoder. In this way, the final transmitted sequence of a systematic codeword becomes $\{\mathbf{D}, \mathbf{q}^{(1)}, \mathbf{P}^{(1)}, \dots, \mathbf{q}^{(M)}, \mathbf{P}^{(M)}\}$. The overall code rate is $\frac{r}{r+M(2^r-r)}$.

Concatenation of non-systematic codes: The encoder output of a non-systematic concatenated code is $\{\tilde{\mathbf{D}}^{(m)}, \mathbf{q}^{(m)}, \mathbf{P}^{(m)}\}$, $\forall m$. All coded bits from the M ZH component codes are transmitted (which is necessary since there are no repeated systematic bits). The final transmitted sequence of a non-systematic

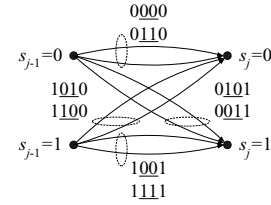


Fig. 2. An example of the j th section of the trellis based on a ZH code with $r = 2$.

codeword is $\{\tilde{\mathbf{D}}^{(1)}, \mathbf{q}^{(1)}, \mathbf{P}^{(1)}, \dots, \tilde{\mathbf{D}}^{(M)}, \mathbf{q}^{(M)}, \mathbf{P}^{(M)}\}$. The code rate of this non-systematic concatenated code is $\frac{r}{M2^r}$.

Concatenation of punctured codes: We can puncture the common bits $\mathbf{q}^{(m)}$, $\forall m$, (the first bit in each segment) of both systematic and non-systematic ZH code. The rates for concatenated punctured systematic and non-systematic ZH codes are $\frac{r}{r+M(2^r-r-1)}$ and $\frac{r}{M(2^r-1)}$, respectively.

D. Decoding Algorithms

1) **Low-Complexity APP Hadamard Decoding:** Denote $\mathbf{x} = [x(0), \dots, x(2^r-1)]$ as the received sequence of channel corrupted Hadamard codeword $\mathbf{c} = [c(0), \dots, c(2^r-1)]$. The log-likelihood-ratios (LLRs) of the coded bits from the APP decoding over $\{+1, -1\}$ are obtained by

$$L(i) = \log \frac{P(c(i)=+1|\mathbf{x})}{P(c(i)=-1|\mathbf{x})} = \log \frac{P(\mathbf{x}|\mathbf{c}(i)=+1)P(\mathbf{c}(i)=+1)}{P(\mathbf{x}|\mathbf{c}(i)=-1)P(\mathbf{c}(i)=-1)}$$

$$= \log \frac{\sum_{\mathbf{c} \in \{\pm \mathbf{h}^j\}: c(i)=+1} P(\mathbf{x}|\mathbf{c})P(\mathbf{c})}{\sum_{\mathbf{c} \in \{\pm \mathbf{h}^j\}: c(i)=-1} P(\mathbf{x}|\mathbf{c})P(\mathbf{c})}, \quad i = 0, \dots, 2^r-1. \quad (3)$$

Denote $H(i, j)$ as the (i, j) -th entry of the Hadamard matrix \mathbf{H} . Thus, for $c(i)=+1$, we have $\mathbf{c} = \mathbf{h}^j$ with $H(i, j)=+1$ or $\mathbf{c} = -\mathbf{h}^j$ with $H(i, j)=-1$; similarly for $c(i)=-1$. Assume the coded bits are transmitted through an AWGN channel with noise variance $\sigma^2 = \frac{N_0}{2}$. Given the *a priori* LLR $L_{apr}(i) = \log \frac{P(c(i)=+1)}{P(c(i)=-1)}$, we obtain

$$L(i) = \log \frac{\sum_{\mathbf{h}^j \in \{\mathbf{H}: H(i, j)=\pm 1\}} \exp(-\|\pm \mathbf{h}^j - \mathbf{x}\|^2 / 2\sigma^2) P(\mathbf{c}=\pm \mathbf{h}^j)}{\sum_{\mathbf{h}^j \in \{\mathbf{H}: H(i, j)=\mp 1\}} \exp(-\|\pm \mathbf{h}^j - \mathbf{x}\|^2 / 2\sigma^2) P(\mathbf{c}=\pm \mathbf{h}^j)}$$

$$= \log \frac{\sum_{\mathbf{h}^j \in \{\mathbf{H}: H(i, j)=\pm 1\}} \gamma(\pm \mathbf{h}^j)}{\sum_{\mathbf{h}^j \in \{\mathbf{H}: H(i, j)=\mp 1\}} \gamma(\pm \mathbf{h}^j)}, \quad (4)$$

where $\gamma(\pm \mathbf{h}^j) \triangleq \exp(\frac{1}{2} \langle \pm \mathbf{h}^j, \frac{2\mathbf{x}}{\sigma^2} + L_{apr} \rangle)$ and $\langle \cdot, \cdot \rangle$ denotes the inner product. Direct calculation of the LLR in (4) has a high computational complexity, $\mathcal{O}(2^{2r})$. The *a posteriori* probability fast Hadamard transform (APP-FHT) developed in [13] can be employed to reduce the complexity based on the butterfly graph of the Hadamard matrix.

2) **Low-Complexity APP Decoding of a ZH Code:** The encoding of a ZH code defined in Section II-B is a Markov process and is related to the information bits only through the first bit in the k th segment. Consequently, the APP decoding of a ZH code can be accomplished using the following two-way algorithm. We consider a ZH code with K segments.

(i) **Preparation:** Let $x_k(i)$ be the noisy observation of $c_k(i)$ (the i th bit in \mathbf{c}_k). The decodings involved in each segment are

based on the algorithm developed in [13] using the *a priori* LLRs $\tilde{L}_k(i)$ for $\{c_k(i)\}$ defined by $\tilde{L}_k(i)=2x_k(i)/\sigma^2, \forall i, k$.

(ii) *Forward recursion*: For $k = 1, \dots, K$, apply APP decoding (4) to the last bit in the k th segment. Then update the *a priori* LLR of the first bit in the $(k+1)$ th segment by adding the *a posteriori* LLR of the last bit in the k th segment.

(iii) *Backward recursion*: Keep the updating for the first bit in every segment as in the Forward Recursion. For $k = K, \dots, 1$, apply APP decoding employing FHT and APP-FHT to the k th segment to obtain the output LLRs. Then update the *a priori* LLR of the last bit in the $(k-1)$ th segment by adding the extrinsic LLR of the first bit in the k th segment.

The overall complexity of above decoding algorithm is then about $r \times n + 9n$ additions per segment per iteration [15]. (We have ignored operations such as updating the first and last bits.) Since each segment carries r bits of information, the about complexity is equivalent to $n + 9n/r$ additions per information bit per iteration, which is quite moderate. The reduced-input FHT technique discussed in [13] can also be used for further cost reduction.

3) *Decoding of Concatenated ZH Codes*: The iterative decoder for a concatenated zigzag Hadamard code with M component codes is similar to that of the concatenated tree decoder discussed in [14]. The decoder consists of M iterative local decoders. The LLRs of the information bits are exchanged between two adjacent local decoders during decoding.

III. PERFORMANCE ANALYSIS

A. EXIT Chart Analysis

The extrinsic information transfer (EXIT) chart [16] is an efficient tool for assessing the asymptotic performance (infinite code length) and the convergence behavior of trellis codes. We next employ this technique to analyze the performance of the concatenated ZH codes.

1) *Threshold Analysis*: A concatenated code with M component codes usually requires an M -dimensional EXIT plot. However, when all of the component codes are identical, the issue can be greatly simplified, as discussed below.

Denote $\mathbf{Z}^{(m)}$ as the channel observations of the m th component code and $\mathbf{A}^{(m)}$ as the input *a priori* LLRs to the m th component code for the information bits \mathbf{D} . Initially, set $\mathbf{A}^{(m)}$ to zero. For each iteration, the extrinsic LLRs $\mathbf{E}^{(m)}$ of \mathbf{D} are obtained from the APP decoding based on $\mathbf{Z}^{(m)}$ and $\mathbf{A}^{(m)}$. $\mathbf{A}^{(m)}$ is updated as $\mathbf{A}^{(m)} = \sum_{m' \neq m} \mathbf{A}^{(m \leftarrow m')}$, where $\mathbf{A}^{(m \leftarrow m')}$ is obtained from $\mathbf{E}^{(m')}$ after interleaving.

Denote $I(\mathbf{D}; \mathbf{A}^{(m \leftarrow m')})$ as the mutual information between \mathbf{D} and $\mathbf{A}^{(m \leftarrow m')}$, and $I(\mathbf{D}; \mathbf{E}^{(m)})$ the mutual information between \mathbf{D} and $\mathbf{E}^{(m)}$. Because all component codes are identical and all $\mathbf{Z}^{(m)}$ are statistically equivalent, for all m, m' , $I(\mathbf{D}; \mathbf{A}^{(m \leftarrow m')})$ are equal during a given iteration, so are $I(\mathbf{D}; \mathbf{E}^{(m)})$. Hence, we can define $I(\mathbf{D}; \mathbf{A}^{(m \leftarrow m')}) = I_A$ and $I(\mathbf{D}; \mathbf{E}^{(m)}) = I_E$. We now consider an example of a concatenated systematic ZH code with common bits punctured. In this example, $M=3$ and $r=8$. The code rate is 0.0107. The EXIT chart of I_E versus I_A on a two-dimensional plane is

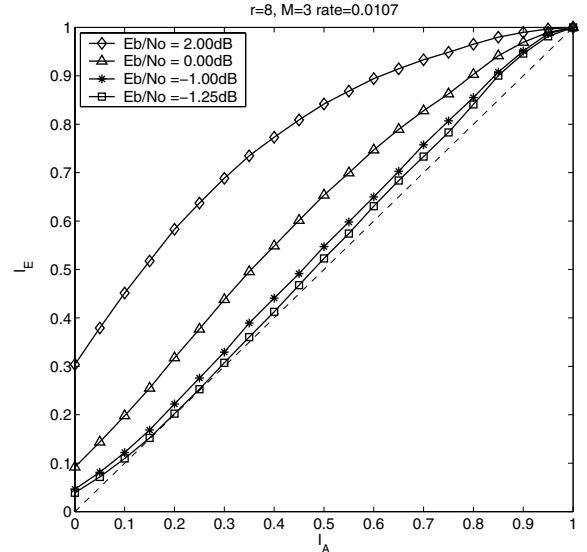


Fig. 3. EXIT chart for a punctured systematic concatenated ZH code with $r = 8$ and $M = 3$.

plotted in Fig. 3. We can clearly see the evolution of I_E . When the extrinsic mutual information evolves to one it indicates the density converges to infinity and the error probability approaches zero. When E_b/N_0 is below a certain value, the EXIT curves intersect with the line $y=x$ before reaching one. In this case, a decoding error floor occurs. The E_b/N_0 value where the EXIT curve is just tangent to the diagonal line $y = x$ is called *threshold*. The EXIT analysis can be validated through the simulations of long codes. The simulation results will be given in Section IV.

Systematic ZH Codes							
order and rate R	$r=2$	$r=3$	$r=4$	$r=5$	$r=6$	$r=7$	$r=8$
Capacity E_b/N_0 (dB)	0.400	0.200	0.108	0.060	0.034	0.019	0.0107
E_b/N_0 EXIT (dB)	-0.24	-0.95	-1.25	-1.41	-1.48	-1.52	-1.54
E_b/N_0 Simu. (dB)	0.90	N/A	-0.60	N/A	-1.10	N/A	-1.25
E_b/N_0 Simu. (dB)	0.97	N/A	-0.44	N/A	-0.98	N/A	-1.15
Non-systematic ZH Codes							
order and rate R	$r=2$	$r=3$	$r=4$	$r=5$	$r=6$	$r=7$	$r=8$
Capacity E_b/N_0 (dB)	0.222	0.143	0.089	0.054	0.032	0.018	0.0105
E_b/N_0 EXIT (dB)	-0.89	-1.14	-1.31	-1.43	-1.49	-1.53	-1.54
E_b/N_0 Simu. (dB)	0.20	-0.20	-0.45	-0.75	-1.00	-1.20	-1.20
E_b/N_0 Simu. (dB)	0.26	-0.10	-0.41	-0.69	-0.95	-1.12	-1.11
Turbo Hadamard Codes							
order and rate R	$r=2$	$r=3$	$r=4$	$r=5$	$r=6$	$r=7$	$r=8$
Capacity E_b/N_0 (dB)	0.250	0.167	0.100	0.058	0.033	0.019	0.0106
E_b/N_0 Simu. (dB)	0.95	0.07	-0.38	-0.70	-0.95	-1.18	-1.13

TABLE I

E_b/N_0 THRESHOLD PERFORMANCE OF CONCATENATED ZH CODES AND TURBO HADAMARD CODES WITH $M = 3$ FOR AWGN CHANNELS.

Table I lists the E_b/N_0 thresholds for both systematic and non-systematic codes. Interestingly, some systematic concatenated codes do not have the threshold. In these cases, the EXIT curves cannot approach one. Therefore, they must have an intersection with the line $y=x$. An example for $r=5$ and $M=3$ is shown in Fig. 4. We find that this happens for all systematic codes with the odd Hadamard orders. In the following, we will provide an explanation for this phenomenon.

2) *Recursiveness of Systematic and Non-systematic ZH Codes*: We first introduce some definitions. By “weight” we always mean Hamming weight. We will say that a ZH code is convolutional-like. A convolutional-like code can be extended

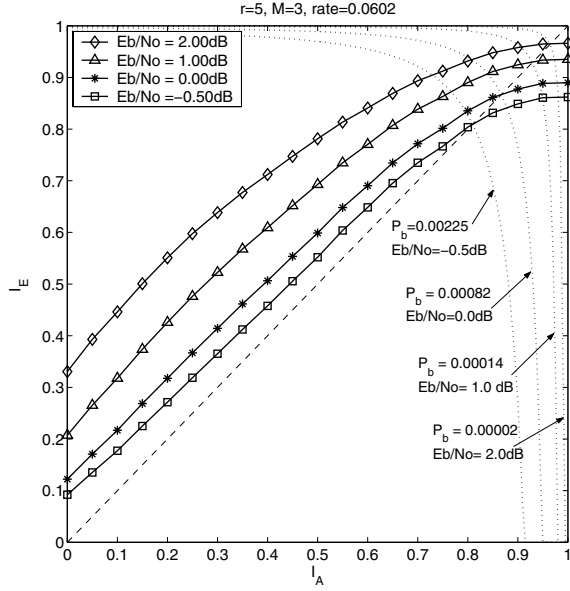


Fig. 4. EXIT chart for a punctured systematic concatenated ZH code with $r = 5$ and $M = 3$.

indefinitely with a regular pattern with rate independent of its length. It is true for the ZH code defined in Fig. 1 (with the first bit in the first segment ignored). A binary convolutional-like code is said to be weight-recursive if any information sequence with Hamming weight one will produce a codeword with Hamming weight $\rightarrow \infty$ when its length $\rightarrow \infty$.

As an example, the convolutional code used in [2] is weight recursive. The weight-recursive property is the necessary condition for a code to achieve error free performance in an AWGN channel (assuming finite transmission energy) since otherwise, there are always codewords with finite weight even when the length goes to infinity. It is easy to verify that if the minimum Hamming weight of a linear code is finite then it cannot achieve error-free performance. Note that here error-free performance does not imply channel capacity, but it implies the existence of a threshold.

Note that the weight-recursive property is not a sufficient condition for error-free performance, since there may be codewords with information sequences with weight larger than one. However, if several weight-recursive codes are concatenated using random interleavers, then the resultant code may achieve error-free performance in large probability. On the other hand, the concatenation of several non-weight-recursive codes will still produce a non-weight-recursive code and so it cannot achieve error-free performance. Interested readers are referred to [17].

For the ZH code, we have following theorem.

Theorem 3.1: The non-systematic ZH codes with any order $r > 1$ and the systematic ZH codes with even order are weight recursive. The systematic ZH codes with odd order are not weight recursive.

Proof: We only show that the systematic ZH codes with even order are weight recursive by induction. Others can be proved similarly. We prove the following relationship for a

systematic ZH code with even r :

$$c_{k+1}(0) = c_k(0) \oplus d_k(1) \oplus d_k(2) \oplus \cdots \oplus d_k(r). \quad (5)$$

Based on (5), it is easy to verify that the weight of an infinitely long code will approach infinite when there is only one non-zero input bit. Based on the basic definitions, we have $c_{k+1}(0) = c_k(2^r - 1)$. So for systematic code, we have $c_k(2^{j-1}) = d_k(j)$ for $j = 0, 1, \dots, r-1$. Then, to prove (5), it suffices to show

$$c_k(2^r - 1) = c_k(0) \oplus c_k(1) \oplus c_k(2) \oplus \cdots \oplus c_k(2^{r-1}). \quad (6)$$

This can be proved by induction. First, we examine $r = 2$ case. Denote \overline{M} as the Hadamard matrix in binary $\{0, 1\}$ form. The Hadamard codeword matrix is given by

$$M_4 = \begin{bmatrix} 0 & 0 & 0 & 0 \\ 0 & 1 & 0 & 1 \\ 0 & 0 & 1 & 1 \\ 0 & 1 & 1 & 0 \end{bmatrix} \text{ and } \overline{M}_4 = \begin{bmatrix} 1 & 1 & 1 & 1 \\ 1 & 0 & 1 & 0 \\ 1 & 1 & 0 & 0 \\ 1 & 0 & 0 & 1 \end{bmatrix}, \quad (7)$$

where \overline{M} is denoted as binary complementary matrix of M . It is easily verified that (6) is satisfied by M_4 and \overline{M}_4 . Now assume (6) is also true for the Hadamard matrix with order $r = m$, i.e., M_n , where $n = 2^m$, given by

$$c_k(2^m - 1) = c_k(0) \oplus c_k(1) \oplus \cdots \oplus c_k(2^{m-1}). \quad (8)$$

Then, the Hadamard matrix with order $r = m + 2$ is given by

$$M_{4n} = \begin{bmatrix} M_n & M_n & M_n & M_n \\ M_n & \overline{M}_n & M_n & \overline{M}_n \\ M_n & M_n & \overline{M}_n & \overline{M}_n \\ M_n & \overline{M}_n & \overline{M}_n & M_n \end{bmatrix}. \quad (9)$$

From the above matrix, we can find the following relationship for all the codewords with length 2^{m+2} , given by

$$c_k(2^{m+2} - 1) \oplus c_k(2^m - 1) = c_k(2^m) \oplus c_k(2^{m+1}). \quad (10)$$

Therefore, we have

$$\begin{aligned} c_k(2^{m+2} - 1) &= c_k(2^m - 1) \oplus c_k(2^m) \oplus c_k(2^{m+1}) \\ &= c_k(0) \oplus c_k(1) \oplus \cdots \oplus c_k(2^{m-1}) \\ &\quad \oplus c_k(2^m) \oplus c_k(2^{m+1}). \end{aligned} \quad (11)$$

Similarly we can prove this for \overline{M}_{4n} . ■

3) *Error Probability Estimation:* Although there is no threshold for the systematic codes with odd orders, the converged bit error probability P_b can be estimated from the intersection points in the EXIT charts [16], given by

$$P_b \approx Q\left(\frac{1}{2}\sqrt{8R\frac{E_b}{N_0} + J^{-1}(I_A)^2 + J^{-1}(I_E)^2}\right), \quad (12)$$

where $Q(x) = \frac{1}{\sqrt{2\pi}} \int_{-\infty}^x e^{-\frac{t^2}{2}} dt$; and the function $J(\sigma)$ is defined by $J(\sigma) \triangleq 1 - \int_{-\infty}^{\infty} \frac{e^{-\frac{y-\sigma^2/2}{2\sigma^2}}}{2\sqrt{\pi x}} \log_2(1+e^{-y}) dy$. The decoding of concatenated ZH code converges at the intersection point of the EXIT curve and the diagonal line $y=x$, where

$I_E=I_A$. Recall that we have M concatenated component codes and the EXIT chart we considered is mapped from M -dimension to 2-dimension because of the identical component codes. Therefore, we have

$$\begin{aligned} P_b &\approx Q\left(\frac{1}{2}\sqrt{8R\frac{E_b}{N_0}+(M-1)\cdot J^{-1}(I_A)^2+J^{-1}(I_E)^2}\right) \\ &= Q\left(\frac{1}{2}\sqrt{8R\frac{E_b}{N_0}+M\cdot J^{-1}(I_x)^2}\right), \end{aligned} \quad (13)$$

where I_x denotes the extrinsic mutual information at the crossing point, $I_x=I_A=I_E$. Some contours of error probability for different E_b/N_0 values are illustrated in Fig. 4. In Section IV, we will compare the estimated bit error probabilities from the EXIT charts with simulation results.

B. Distance Spectrum and Union Bound

The union bound is an upper bound for the code error probability. The union bound can be obtained through the distance spectrum analysis. Define the *input-output weight enumerating function* (IOWEF) of a code C [18] as $A^C(W, Y)=\sum_{w,y} A_{w,y} W^w Y^y$, where $A_{w,y}$ denotes the number of weight- y codewords generated by weight- w information words. Notice that for a conventional code, $A_{w,y}$ is usually an integer. For a concatenated code, $A_{w,y}$ is defined in the form of an ensemble weight distribution, which is a probability measure averaged over all possible interleavers [17], [18].

Here we consider only the un-punctured codes. If the common bit of a Hadamard codeword is not punctured, there are only three possible weights: 0, 2^{r-1} , and 2^r associated with each segment (i.e., the weight of a length- 2^r Hadamard codeword). Therefore we only need to consider the terms associated with those y that are multiples of 2^{r-1} (for a detailed discussion, see [13]). Consequently, the IOWEF approach can be efficiently evaluated [17]. The bit error probability of C is upper-bounded by

$$P_b(e) \leq \sum_y \sum_w \frac{w}{N} A_{w,y} Q\left(\sqrt{2yR\frac{E_b}{N_0}}\right), \quad (14)$$

where N is the number of information bits and R is the code rate of C .

IV. NUMERICAL RESULTS

This section provides the performance results of concatenated ZH codes from computer simulations. We first present results of long codes to demonstrate their capacity approaching performance. Then, we present the performance of short codes.

A. Performance of Long Concatenated ZH Codes

Fig. 5 illustrates the BER performance of the punctured systematic concatenated ZH codes. The interleaver length, N is set to be divisible by the Hadamard order r . The maximum number of decoding iterations is 50. It is seen from Fig. 5 that all codes with even Hadamard orders have waterfalls in the BER curves. The E_b/N_0 thresholds at $\text{BER}=10^{-5}$ are listed in Table I and are compared with the threshold results from

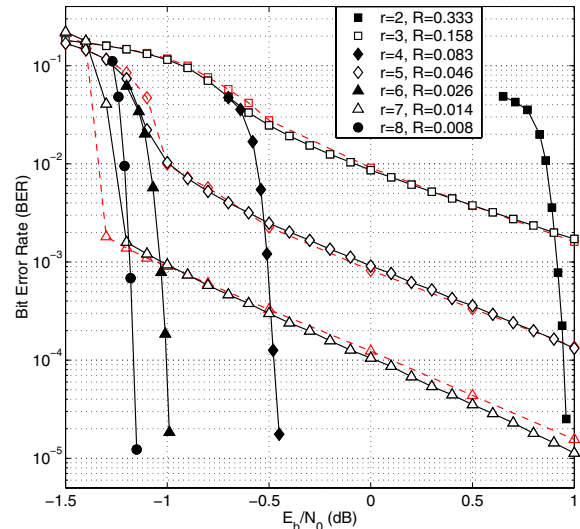


Fig. 5. BER performance of concatenated punctured systematic ZH codes with $M = 3$, the interleaver length $N \approx 65536$. Dashed lines represent the approximated bit error probability from EXIT charts. The solid lines represent the BER performance from computer simulations.

the EXIT analysis and the capacity bound. It is seen that the simulation results matched very well with the EXIT analysis.

It is also seen from Fig. 5 that the systematic codes with odd r do not have thresholds. The reason is explained in the previous section. The converged error probabilities estimated from the EXIT chart are illustrated by the dashed curves. It is seen that the estimated BER performance matches very well with the simulations. These demonstrate that the EXIT chart is a useful tool to analyze the asymptotic performance of the concatenated ZH codes with large code length. The error floor of concatenated ZH codes can be explained by Theorem 3.1, which is due to non-recursiveness of the systematic ZH codes with odd r .

The BER performance of non-systematic codes and the turbo Hadamard codes is illustrated in Fig. 6. The rate of turbo Hadamard codes is $\frac{r}{r+M(2^r-r)}$. All non-systematic codes with different order r exhibit a sharp waterfall. The E_b/N_0 thresholds are also summarized in Table I. From Fig. 6, the non-systematic ZH codes have better performance for small r , but the turbo-Hadamard codes become better for large r .

B. Performance of Short Concatenated ZH Codes

The performances of systematic ZH codes are very similar to that of the non-systematic ZH codes with even r . Therefore, we only present results for the non-systematic ZH codes. For short codes, we set $N \approx 200$ and $M=4$. The maximum iteration number is 30. The performance of the concatenated punctured non-systematic ZH codes and that of the turbo Hadamard codes is compared in Fig. 7. The generator polynomial of the turbo-Hadamard code is $\frac{1}{1+D}$. We can see from Fig. 7 that the non-systematic ZH codes slightly outperform the turbo Hadamard codes for the same order (although the rates of the former is slightly lower).

Based on the discussion in Section II, the decoding complexity of the concatenated ZH code with $r = 4, M = 4$ ($R = 1/12$) is about $4 \times (16 + 9 \times 16/4) = 208$ additions

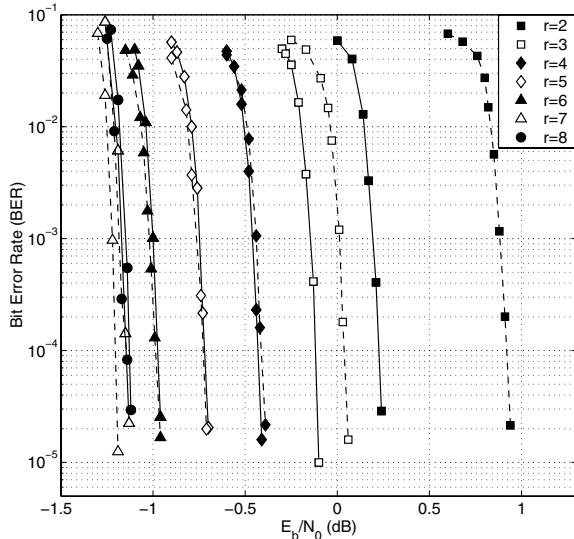


Fig. 6. BER performance of concatenated punctured non-systematic ZH codes (solid lines) and turbo Hadamard codes (dashed lines) with $M = 3$, the interleaver length $N \approx 65536$.

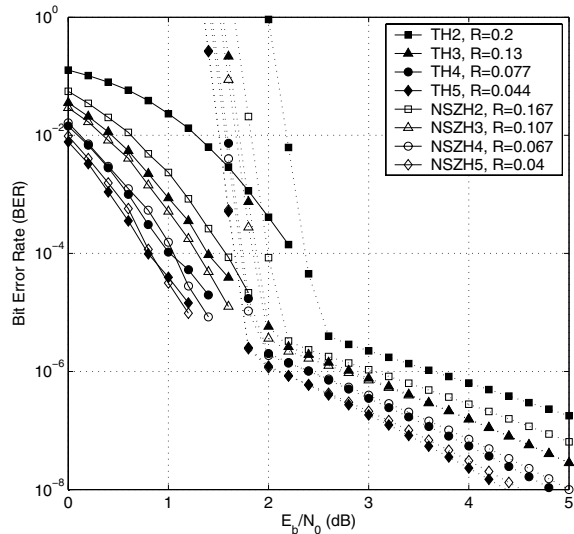


Fig. 7. Performance comparisons of punctured non-systematic concatenated ZH (NSZH) codes and turbo Hadamard (TH) codes: $N \approx 200$, $M = 4$. The number after "NSZH" and "TH" in the legend represents the Hadamard order r . The dashed lines represent upper bounds. The solid lines represent the BER performance from computer simulations.

per information bit per iteration. As shown in [13], the turbo-Hadamard codes with $r = 3$, $M = 4$ ($R = 1/7.7$) involves approximately total 241 operations (including additions and multiplications) per information bit per iteration. Therefore, the proposed low-rate concatenated ZH codes have lower decoding complexity.

V. CONCLUSIONS

This paper presents a new class of low-rate error correction codes, the concatenated zigzag Hadamard codes. We have presented the EXIT chart and union bound analyses for infinite-length and finite-length codes, respectively. The results show that a rate-0.0107 concatenated zigzag Hadamard

code performs only 0.44dB away from the ultimate low-rate Shannon limit. Compared with the low-rate turbo Hadamard codes, the proposed concatenated ZH codes offer similar performance but with much lower encoding and decoding complexities.

REFERENCES

- [1] C. E. Shannon, "A mathematical theory of communication," *Bell System Tech. J.*, vol. 27, pp. 379–423 and 623–656, July and Oct. 1948.
- [2] C. Berrou, A. Glavieux, and P. Thitimajshima, "Near shannon limit error-correcting and decoding: Turbo codes," in *Proc. of Int. Conf. Commun. (ICC)*, Geneva, Switzerland, May 1993, pp. 1064–1070.
- [3] P. Komulainen and K. Pehkonen, "Performance evaluation of super-orthogonal turbo codes in AWGN and flat Rayleigh fading channels," *IEEE J. Select. Areas Commun.*, vol. 16, no. 2, pp. 196–205, Feb. 1998.
- [4] M. Bingeman and A. K. Khandani, "Symbol based turbo codes," *IEEE Commun. Lett.*, vol. 3, no. 10, pp. 285–287, Oct. 1999.
- [5] H. Jin and R. J. McEliece, "RA codes achieve AWGN channel capacity," in *Proc. Int. Symp. Applied Algebra & Error-Correcting Codes*, Honolulu, HI, Nov. 1999, pp. 14–19.
- [6] R. G. Gallager, "Low-density parity check codes," *IRE Trans. Inform. Theory*, vol. 39, no. 1, pp. 37–45, Jan. 1962.
- [7] D. J. C. MacKay and R. M. Neal, "Near shannon limit performance of low density parity check codes," *Elect. Lett.*, vol. 33, no. 6, pp. 457–458, Mar. 1997.
- [8] S. Y. Chung, G. D. Forney, T. J. Richardson, and R. Urbanke, "On the design of low-density parity-check codes within 0.0045 dB of the shannon limit," *IEEE Commun. Lett.*, vol. 5, no. 2, pp. 58–60, Feb. 2001.
- [9] O. Wintzell, M. Lentmaier, and K. Zigangirov, "Asymptotic analysis of superorthogonal turbo codes," *IEEE Trans. Inform. Theory*, vol. 49, no. 1, pp. 253–258, Jan. 2003.
- [10] J. Hamkins and D. Divsalar, "Coupled receiver-decoders for low rate turbo codes," in *Proc. IEEE Int. Symp. Inform. Theory (ISIT)*, Yokohama, Japan, June 2003, p. 381.
- [11] G. Yue, L. Ping, and X. Wang, "Low-rate generalized low-density parity-check codes with Hadamard constraints," in *Proc. IEEE Int. Symp. Inform. Theory (ISIT)*, Adelaide, Australia, Sept. 2005.
- [12] L. Ping, X. Huang, and N. Phamdo, "Zigzag codes and concatenated zigzag codes," *IEEE Trans. Inform. Theory*, vol. 47, no. 2, pp. 800–807, Feb. 2001.
- [13] L. Ping, W. K. Leung, and K. Y. Wu, "Low-rate turbo-Hadamard codes," *IEEE Trans. Inform. Theory*, vol. 49, no. 12, pp. 3213–3224, Dec. 2003.
- [14] L. Ping and K. Y. Wu, "Concatenated tree codes: A low-complexity high-performance approach," *IEEE Trans. Inform. Theory*, vol. 47, no. 2, pp. 791–799, Feb. 2001.
- [15] W. K. Leung, G. Yue, L. Ping, and X. Wang, "Concatenated zigzag Hadamard codes," submitted to *IEEE Trans. Inform. Theory*.
- [16] S. ten Brink, "Convergence behavior of iterative decoded parallel concatenated codes," *IEEE Trans. Commun.*, vol. 49, no. 10, pp. 1727–1737, Oct. 2001.
- [17] S. Benedetto and G. Montorsi, "Unveiling turbo codes: some results on parallel concatenated coding schemes," *IEEE Trans. Inform. Theory*, vol. 42, no. 2, pp. 409–428, Mar. 1996.
- [18] S. Benedetto, D. Divsalar, G. Montorsi, and F. Pollara, "Analysis, design, and iterative decoding of double serially concatenated codes with interleavers," *IEEE J. Select. Area Commun.*, vol. 16, no. 2, pp. 231–244, Feb. 1998.